ASEAN Engineering Journal

Full Paper

OPTIMIZATION OF PROCESS PARAMETERS OF 3D PRINTED POLYLACTIC ACID PARTS USING GENETIC ALGORITHM

Raghavendra BV*, Anandkumar R Annigeri

Department of Mechanical Engineering, JSS Academy of Technical Education, Bengaluru, India-560060

Article history
Received
12 April 2024
Received in revised form
20 August 2024
Accepted
11 September 2024
Published online
31 May 2025

*Corresponding author
bvraghavendra@jssateb.ac.in

Graphical abstract

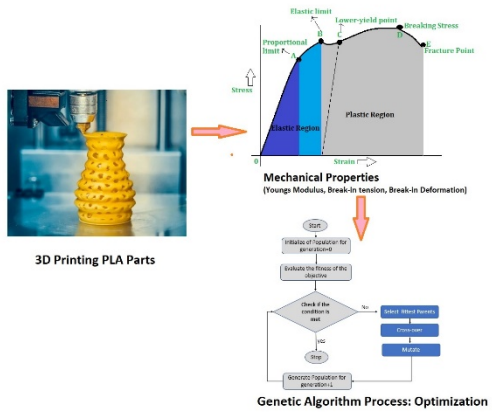

Abstract

In this paper, the optimization of input process parameters of 3D printed parts of Polylactic Acid in Fused Deposition Modeling is studied using a genetic algorithm. The work emphasizes on influence of input process parameters on Young's modulus, breakage tension, and breakage deformation. Optimization of process parameters is studied for single objectives such as Young's modulus, break in tension, and breakage deformation and also optimizing combined three objective functions simultaneously. The regression model is used as a fitness function to optimize the objectives. Built-in functions in MATLAB 'ga' and 'gamultiobj' are applied for optimization of single and multi-objectives respectively. The study reveals that simultaneous optimization of three objectives reduces a 27.27% breakage deformation, 13.7% Young's modulus, and 55.5% break-in tension as compared to optimization of individual objectives.

Keywords: 3D Printed Parts, Optimization, Genetic Algorithm, Single Objective function, Multi Objective function.

1.0 INTRODUCTION

Polylactic Acid (PLA) is a bio-polymer that is produced from plant starches using a sustainable process. It is biodegradable under appropriate conditions and is generally regarded as food-safe since it decomposes back into its lactic acid building blocks, which are non-toxic. The PLA is commonly used in medical devices, food packaging, injection molding, and additive manufacturing (3D printing) applications. The material has a high-strength but brittle plastic and is not ideal for parts subjected to shock loads. It is a biodegradable thermoplastic obtained from totally renewable resources, which decomposes into water, carbon dioxide, and humus [1]. The PLA has better mechanical properties like high stiffness and high strength compared to many synthetic polymers [2] [3] [4]. It has a density of 1.27 g/cm3, tensile strength is 59 MPa, elongation at break is 7 %, elastic modulus of 3500 MPa, shear modulus of 1287 MPa, flexural Strength 106 MPa, Rockwell hardness (HRA) is 88, glass transition temperature is 55°C, melting point 165°C. Some of the advantages of PLA are Biocompatibility, low energy for production, better mechanical properties, food safety, and compostable. The limitations of PLA are hydrophobic material, low thermal resistance, low toughness, and high permeability.

PLA has elongation of 3.1–5.8 % (un-oriented) and 15–160% (oriented) filaments [3] at the break. At temperatures above 200°C, the thermal degradation of PLA leads to hydrolysis, lactide reformation, oxidative main chain scission, and inter- or intra-molecular transesterification reactions. PLA degradation is dependent on time, temperature, low-molecular-weight impurities, and catalyst concentration.

Young's modulus, a material property representing its stiffness or resistance to deformation under stress, significantly influences the 3D printing approach in Fused Deposition Modeling (FDM). Young's modulus varies across different materials viz., PLA, ABS, and PETG used in FDM printing and the knowledge of Young's modulus is crucial in choosing a material for 3D printing based on material selection, print quality, structural integrity, layer adhesion, print settings optimization, and design considerations. Materials with higher Young's modulus are stiffer and less flexible, while those with lower

Young's modulus are more flexible. Understanding and leveraging this material property can help achieve performance characteristics in 3D-printed parts. Gibson et al. [5] conducted a comprehensive overview of FDM, along with the influence of material properties like Young's modulus on the process and final part properties. Hopkinson et al. [6] narrated various aspects of rapid manufacturing, particularly FDM, and discussed how material properties, including Young's modulus, impact the process and applications. Rouf et al. [7] investigated the influence of process parameters of 3D-printed PLA, including how variations in Young's modulus affect the final part properties [8]. Travieso-Rodriguez et al.[9] examined the flexure of PLA parts fabricated with FDM and discussed how variations in Young's modulus due to build orientation and manufacturing strategy impact part performance. The material breakage tension (tensile strength), significantly influences 3D printing using FDM and is crucial for producing high-quality and functional 3D-printed parts. Sandanamsamy et al. [10] investigated how process parameters affect the breakage tension of PLA specimens printed using FDM technology, providing insights into optimizing print settings for improved mechanical properties. Fontana et al. [11] explored how printing parameters impact tensile strength, of PLA samples produced using FDM, through experimental and numerical approaches to analyze the results. Tofail et al. [12] reviewed the various aspects of additive manufacturing, including FDM, and how tensile strength influences the technology's scientific and technological challenges, market uptake, and opportunities. Kumar et al. [13] investigated PLA for different fiber content fabricated using FDM, shedding light on how material composition affects mechanical performance in additive manufacturing. Marșavina et al. [14] studied the tensile strength of PLA parts produced via FDM, providing insights into the performance of FDM-printed parts in various loading conditions. Tünçay [15] investigated how print orientation affects the yield strength of PLA specimens produced using FDM, providing insights into optimizing print orientations for improved performance. Ambade et al.[16] studied the influence of yield strength of PLA and ABS polymers manufactured using FDM, offering insights into parameter optimization for enhanced performance. Khan et al.[17] conducted a review of the effects of yield strength of PLA and ABS parts fabricated using FDM, providing valuable insights into orientation-dependent mechanical behavior. Kumaresan et al. [18] examined yield strength, and microstructural characteristics of PLA and PETG parts produced using FDM, offering insights into the relationship between material properties and print quality. Doshi et al. [19] investigated the influence of print orientation and infill density including yield strength, of parts fabricated using FDM, providing insights into parameter optimization for desired performance.

In the open literature, the following studies on the optimization of 3D printing are available. Kristiawan et al.[20], and Dey & Yodo [21] conducted studies on the optimization of FDM 3D printing parameters, Taguchi, ANOVA, and multi-objective optimization is studied by [22-24]. Raghavendra [25-26] worked on the bi-criteria objective, the effect of cross-over probability on GA. GA is the meta heuristic algorithm based on natural selection. GA process drives biological evolution to search results and find global optimal solutions to problems, both constrained and unconstrained problems of complex in nature. Puttaswamy & Raghavendra [27] worked on the significance of process parameters in the machining of parts.

2.0 METHODOLOGY

GA is an optimization technique inspired by the process of natural selection and genetics. They are used to find solutions to optimization and search problems by mimicking the natural evolution process. In this work optimization of Young's modulus, break in tension, and breakage deformation of 3D printed parts is determined using a genetic algorithm. MATLAB has a powerful optimization function ‘ga’ for one objective and ‘gamultiobj’ for multiple objectives. The built-in function ‘ga’ is to optimize the individual objective such as Young's modulus, break in tension, and breakage deformation. The optimization of three objectives simultaneously is simulated using the ‘gamultiobj’ built-in function available in MATLAB. The experimental data available in [28] is used to develop a multiobjective regression equation for all three objectives viz., Young’s modulus, breakage tension, and breakage deformation.

2.1 Single Objective Optimization using the ‘ga’ Function:

The syntax for optimization of built-in function in MATLAB for single objective ‘ga’ is:

[x, fval] = ga(ObnFcn, nvars, A, b, Aeq, beq, lb, ub, nonlcon, options)
‘X’ is a decision variable that minimizes or maximizes the objective (ObnFcn) function.
‘fval’ is the simulated result of the objective function at ‘x’ decision variable
‘ObnFcn’ is the objective function. Objective functions in this research are maximization of Young's modulus, breakage tension, and minimization of breakage deformation.
‘nvars’ is the number of decision/input process parameters.
‘A’, ‘B’, and ‘Aeq’ ‘beq’ are linear in-equality and equality constraints respectively.
‘lb’ and ‘ub’ are the lower and upper bounds of the decision variables.
‘nonlcon’ is a nonlinear constraint.
options parameter to customize the simulation.
Population Size (PopulationSize): Number of individuals in each generation.
Generations: Number of generation to stop the simulation
Stall Gen Limit (StallGenLimit): ga function stops when the average relative change in best fitness value over StallGenLimit generations is less than the TolFun tolerance.
Selection Function (SelectionFcn): Function used for parent selection.
Crossover Function (CrossoverFcn): Function used for crossover.
Crossover Fraction (CrossoverFraction): Fraction of individuals in the population that undergo crossover in each generation.
Migration Fraction (MigrationFraction): Fraction of the smaller of the two subpopulations that move.
Mutation Function (MutationFcn): Function used for mutation.
Display (Display): Display the details during simulation with the options 'off', 'final', and 'iter'.
Max Generations (MaxGenerations): Number of generations set.
TolFun (TolFun): Tolerance on the objective/output value to terminate the optimization.
Plot Function (PlotFcn): Plot the progress of the simulation
options=gaoptimset('PopulationSize',30, 'Generations',100, 'StallGenLimit',200, 'SelectionFcn', @selectionroulette, 'CrossoverFcn', @crossovertwopoint, 'CrossoverFraction',0.7,

'MigrationFraction',0.2, 'MutationFcn', @mutationadaptfeasible, 'Display', 'iter', 'TolFun', 1e-6, 'PlotFcns',{@gaplotbestf, @gaplotbestindiv, @gaplotstopping}); [x, fval]=ga(ObnFcn, nvars, [ ], [ ] ,[ ], [ ], lb, ub, ConsFcn, IntCon, options);

2.2 Multi-objective Function

The standard function available in Matlab for the optimization of multi objectives 'gamultiobj', to optimize all three objectives simultaneously. This function uses a genetic algorithm to search for a set of solutions that represent a trade-off between the conflicting objectives.

The sintex for multiobjectives is: [x, fval] = gamultiobj(fun, nvars, A, B, Aeq, beq, lb, ub, intcon)

gamultiobj function to find the Pareto optimal solutions.
fun is the multiobjective function to optimize and return each objective function values.
intcon returns the integer values for the column selected
x contains the optimal solutions found by the algorithm.
Equation numbers 1, 2, and 3 are used as functions f (1), f (2) and f (3) respectively
Combined all the three objectives for optimization of multi-objective, fun= [f(1) f(2) f(3)]

3.0 RESULTS AND DISCUSSION

Single objective optimization: The parameters set for single objective is:

Number of Iteration=25;
Number of decision variable/Input process parameters=6
Decision variable with their 'lb' (lower) and 'ub' (upper) bonds are:
Temperature (180° C and 200° C), speed- movement of Nozzle (40 mm/sec and 80mm/sec), thickness of layer (0.1 mm and 0.3 mm), extrusion width (0.55 mm and 0.75 mm), test tube position(Horizontal and Vertical), Infill -Internal fill angle (0° and 90°).
lb= [180 40 0.10 0.55 0 0];
ub=[200 80 0.30 0.75 90 90];
ConsFcn=[];
IntCon=[1,2,5,6]
Options:
Population Size=30,
Generations=100,
Stall Gen Limit=200
CreationFcn: @gacreationuniformint
CrossoverFcn: @crossovertwopoint
SelectionFcn: @selectionroulette
MutationFcn: @mutationadaptfeasible

Eguren et al. [28] modelled a 3D printing process using the DoE approach for PLA material. The regression model/equation (obnFcn) for all the three objectives such as Young's modulus, breakage tension and breakage deformation are further worked and obtain the regression equation using Minitab.

3.1 Regression Model for Young's Modulus (GPa)

ObnFcn= -10.724 + 0.0755 x Temp + 0.046 x Speed -3.3805 x Thickness + 14.7953 x Width + 0.0039 x Position - 0.0118 x Infill Angle - 0.0002 x Temp x Speed - 0.027 x Temp x Thickness - 0.0798 x Temp x Width + 0 x Temp x Position + 0 x Temp x Infill Angle + 0.0371 x Speed x Thickness - 0.0168 x Speed x Width + 0 x Speed x Position + 0 x Speed x Infill Angle + 11.4531 x Thickness x Width - 0.0136 x Thickness x Position - 0.005 x Thickness x Infill Angle - 0.012 x Width x Position + 0.0203 x Width x Infill Angle -0.0001 x Position x Infill Angle .....(1)

The genetic algorithm ('ga' function) is simulated and the results obtained for the optimized process parameters at optimized objective functions of Young's modulus are:

Table 1 Best Process Parameter and Young's Modulus

Best Process Parameters	Value
Temperature (°C)	181
Speed, Movement of Nozzle (mm/sec)	79
Thickness of Layer (mm)	0.29
Extrusion width (mm)	0.75
Test tube position (Degree)	1
Infill angle (Degree)	73
Objective Function :	
Young's Modulus(GPa)	1/0.24480=4.045

The 'ga' function gives the optimization of the parameters by minimizing objective function. However, the study seeks to maximize Young's modulus and hence the result is calculated as a 1/objective function. The figures show the best penalty value as a minimum but reciprocal of the value will be the maximization of the objective function.

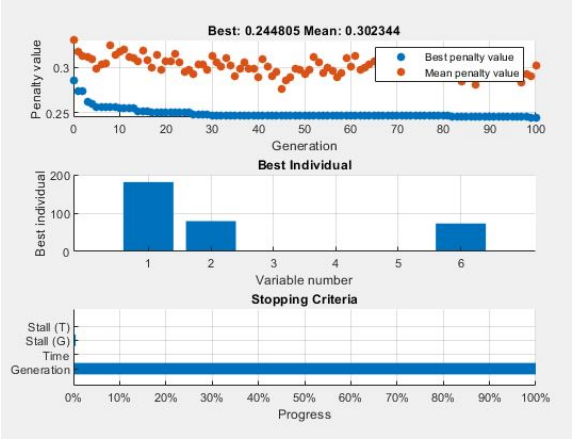

Figure 1 Simulated results of best value, best variable, and stopping details for Young's modulus

In Figures 1-3, following legend is used for computing best individual: (1)Temperature (°C), (2) Speed- movement of Nozzle (mm/sec), (3) Thickness of layer (mm), (4) Extrusion width (mm), (5) Test tube position (angle in degrees), (6) Infill Internal fill angle (degree).

Regression Model for Breakage Tension (MPa)

ObnFcn= -31.43 + 0.074 x Temp - 0.095 x Speed-110.758 x Thickness + 99.584 x Width + 0.712 x Position - 0.222 x Infill Angle + 0 x Temp x Speed + 0.137 x Temp x Thickness - 0.14 x Temp x Width - 0.001 x Temp x Position + 0.001 x Temp x Infill Angle + 0.378 x Speed x Thickness - 0.01 x Speed x Width - 0.001 x Speed

x Position + 0 x Speed x Infill Angle + 145.219 x Thickness x Width - 0.053 x Thickness x Position -0.181 x Thickness x Infill Angle - 0.803 x Width x Position + 0.21 x Width x Infill Angle - 0.001 x Position x Infill Angle .....(2)

Table 2 Best Process Parameter and Breakage Tension

Best Process Parameters	Value
Temperature (^{0}C)	194
Speed, Movement of Nozzle (mm/sec)	79
Thickness of Layer (mm)	0.29
Extrusion width (mm)	0.75
Test tube position (Degree)	0
Infill angle (Degree)	87
Objective Function :	
Breakage Tension (MPa)	1/0.0192=52.084

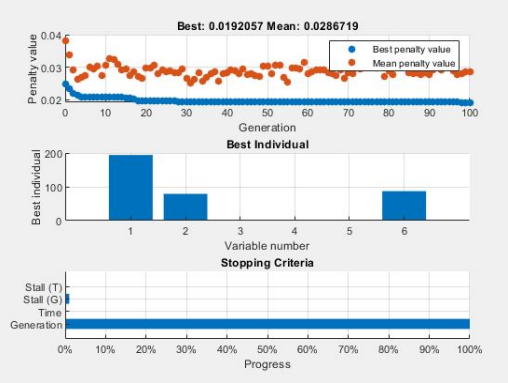

Figure 2 Simulated results of best value, best variable, and stopping details for Breakage Tension

Regression Model for Breakage deformation (mm)=
ObnFun= 0.057734 - 0.000336 x Temp + 0.000684 x Speed + 0.061719 x Thickness – 0.182818 x Width + 0.000089 x Position - 0.000089 x Infill Angle – 0.000004 x Temp x Speed – 0.000469 x Temp x Thickness + 0.001094 x Temp x Width + 0.000002 x Temp x Position + 0 x Temp x Infill Angle + 0.000234 x Speed x Thickness +0.000078 x Speed x Width -0.000002 x Speed x Position + 0.000001 x Speed x Infill Angle + 0.046875 x Thickness x Width + 0.000035 x Thickness x Position -0.000243 x Thickness x Infill Angle - 0.000174 x Width x Position + 0.000104 x Width x Infill Angle +0 x Position x Infill Angle ….(3)

Table 3 Best Process Parameter and Breakage Deformation

Best Process Parameters	Value
Temperature (^{0}C)	200
Speed, Movement of Nozzle (mm/sec)	41
Thickness of Layer (mm)	0.29
Extrusion width (mm)	0.75
Test tube position (Degree)	90
Infill angle (Degree)	14
Objective Function :	
Breakage Deformation (mm)	1/22.62=0.044

The algorithm is run for 100 generations as shown above Figures 1, 2, and 3 indicating the best penalty (minimum) values for all the objective functions. The objective values obtained are, minimum penalty value is 0.244805 and the maximization of this is 1/0.244805= 4.08 GPa for young modulus as shown in Figure 1, minimum penalty value is 0.0.0192 and the maximization of this is 1/0.0192= 52.08 MPa for the breakage tension shown in Figure 2 and, minimum penalty value is 22.628 and the maximization of this is 1/22.628= 0.044 mm for the breakage deformation as shown in Figure 3. The optimum process parameter at the objective function is listed in Tables 1, 2, and 3.

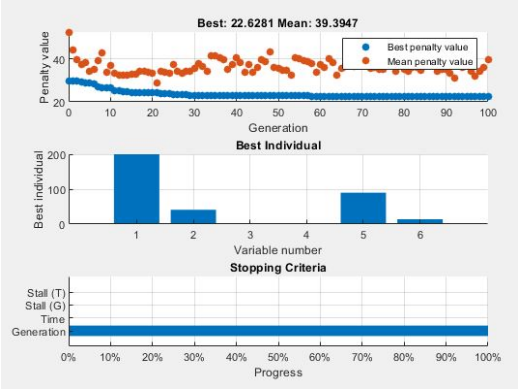

Figure 3 Simulated results of best value, best variable, and stopping details for breakage deformation

Multi-objective function: Input parameters and options used for optimizing multi-objective function for equation numbers 1, 2, and 3 are presented below.

Input parameters:
nvars=6;
A=[], B=[], Aeq=[], beq=[]
lb=[180 40 0.10 0.55 0 0]
ub=[200 80 0.30 0.75 90 90]

Options:
PopulationSize_Data= 30 ,
MaxGenerations_Data=100
MaxStallGenerations_Data=10
FunctionTolerance_Data=0
ConstraintTolerance_Data=0
intcon=[1,2,5,6]
[x, fval] = gamultiobj(fun, nvars, A, B, Aeq, beq, lb, ub, PopulationSize_Data,MaxGenerations_Data, MaxStallGenerations_Data, FunctionTolerance_Data, ConstraintTolerance_Data, intcon);

The simulation stopped at the 70th generation because the average change in the spread of Pareto solutions is less than the Function Tolerance. The optimal simulated result for multi-objective functions such as Young's modulus, breakage tension, and breakage deformation and the process parameters are presented in Table 4 with 70 generation details.

At the 68th generation, the optimum process parameters indicate a minimum breakage deformation of 0.0032 mm and a maximum breakage tension of 23.177 Mpa with the maximum Young's modulus of 2.8048 GPA. Maximum Young's modulus at 16th generation is 3.5252 with the breakage tension 17.3764 Mpa and breakage deformation 0.0057 mm. Three-dimensional

Table 2 Optimal Solution

S No.	Temperature (Degree C)	Speed (mm/sec)	Thickness (mm)	Extrusion width (mm)	Test tube position (degree)	Infill Angle (degree)	Youngs Modulus (Gpa)	Breakage tension (Mpa)	Breakage deformation (mm)
1	180	80	0.1404	0.5503	90	90	1.9639	14.6346	0.0277
2	180	63	0.2899	0.5506	90	90	1.6731	16.4741	0.0285
3	180	40	0.3000	0.5500	32	90	2.2998	21.3996	0.0123
4	180	41	0.2949	0.5500	18	90	2.5385	22.2165	0.0085
5	180	40	0.300	0.5501	3	90	2.7577	23.0188	0.0040
6	180	77	0.2326	0.5559	82	90	2.0104	16.2711	0.0266
7	181	63	0.1455	0.5504	18	61	2.9479	21.2615	0.0120
8	181	66	0.1069	0.5500	4	29	3.1613	19.7348	0.0085
9	185	79	0.1064	0.5500	18	25	3.1847	18.4791	0.0116
10	180	59	0.2976	0.5518	90	90	1.6208	16.8421	0.0285
11	180	68	0.2933	0.5506	90	90	1.7270	16.0642	0.0284
12	180	40	0.3000	0.5503	29	90	2.3488	21.6042	0.0114
13	194	67	0.1329	0.5502	1	34	3.3795	20.9642	0.0074
14	180	73	0.1743	0.5503	11	55	3.0944	21.0111	0.0113
15	189	80	0.1000	0.5500	0	0	3.3832	17.2589	0.0068
16	200	80	0.1000	0.5500	0	0	3.5252	17.3764	0.0057
17	182	80	0.1130	0.5502	85	83	2.1405	15.2232	0.0266
18	180	40	0.3000	0.5500	26	90	2.3946	21.7347	0.0106
19	181	78	0.1313	0.5503	5	23	3.2371	19.1354	0.0096
20	180	49	0.2934	0.5505	74	90	1.7564	18.6048	0.0244
21	181	67	0.1177	0.5505	21	52	2.9711	20.3819	0.0127
22	192	80	0.1006	0.5501	0	0	3.4223	17.3146	0.0065
23	181	70	0.2967	0.5506	87	83	1.8793	16.6643	0.0280
24	181	60	0.2986	0.5508	86	90	1.7020	17.0392	0.0276
25	181	80	0.1015	0.5502	0	0	3.2815	17.225	0.0077
26	183	80	0.1010	0.5500	30	72	2.8864	19.3115	0.0152
27	186	79	0.1072	0.5500	0	13	3.3319	18.2479	0.0075
28	195	80	0.1014	0.5502	0	2	3.4591	17.5140	0.0063
29	180	40	0.3000	0.5500	11	90	2.6312	22.5660	0.0063
30	180	41	0.2998	0.5500	19	90	2.5171	22.1173	0.0087
31	180	48	0.2949	0.5504	55	90	2.0408	19.8620	0.0193
32	181	40	0.2918	0.5507	47	90	2.0947	20.7993	0.0167
33	182	53	0.1825	0.5501	2	47	3.0884	22.0066	0.0076
34	183	66	0.1294	0.5503	18	43	3.0517	20.4341	0.0120
35	183	72	0.1337	0.5504	40	54	2.8300	19.4377	0.0171
36	183	80	0.1009	0.5501	43	79	2.7019	18.5166	0.0181
37	180	40	0.3000	0.5500	16	90	2.5523	22.2884	0.0077
38	180	41	0.2949	0.5500	5	90	2.7427	22.9485	0.0048
39	180	64	0.1146	0.5505	62	82	2.3311	18.9537	0.0221
40	181	43	0.2995	0.5509	90	90	1.4398	18.0503	0.0289
41	180	40	0.2953	0.5511	6	90	2.7202	23.0251	0.0050
42	180	40	0.3000	0.5500	24	90	2.4262	21.8465	0.0100
43	180	40	0.3000	0.5500	86	90	1.4477	18.3997	0.0276
44	180	44	0.2949	0.5501	38	90	2.2598	21.0187	0.0144
45	180	44	0.2986	0.5504	63	90	1.8623	19.5266	0.0213
46	180	49	0.2940	0.5506	90	90	1.5046	17.5727	0.0287
47	180	50	0.2938	0.5502	86	90	1.5778	17.7294	0.0276
48	180	51	0.2833	0.5506	90	90	1.5465	17.5014	0.0287
49	180	56	0.2981	0.5500	90	90	1.5781	16.9574	0.0285
50	180	67	0.1343	0.5502	7	30	3.1360	20.0293	0.0096
51	180	69	0.2844	0.5505	67	90	2.1059	17.9251	0.0232
52	180	72	0.2457	0.5502	90	90	1.8170	15.7235	0.0283
53	180	75	0.1263	0.5501	28	87	2.7896	20.2787	0.0150
54	180	76	0.2962	0.5507	90	90	1.8184	15.4406	0.0283
55	180	80	0.1572	0.5501	90	90	1.9529	14.6778	0.0278
56	181	70	0.1660	0.5503	80	90	2.0309	16.8044	0.0261
57	181	77	0.1989	0.5503	76	90	2.1145	16.4182	0.0252
58	182	67	0.1286	0.5504	18	51	3.0174	20.5916	0.0121
59	185	72	0.1264	0.5503	27	71	2.9190	20.5298	0.0143
60	180	40	0.2997	0.5502	8	90	2.6797	22.7582	0.0055
61	180	40	0.2998	0.5501	14	90	2.5844	22.4082	0.0072
62	180	40	0.3000	0.5503	25	90	2.4119	21.8274	0.0103
63	180	40	0.3000	0.5503	82	90	1.5122	18.6459	0.0265
64	180	40	0.3000	0.5503	28	90	2.3645	21.6600	0.0112

65	180	40	0.3000	0.5503	37	90	2.2225	21.1573	0.0137
66	180	40	0.3000	0.5500	22	90	2.4576	21.9551	0.0094
67	180	40	0.3000	0.5500	90	90	1.3846	18.1775	0.0287
68	180	40	0.3000	0.5500	0	90	2.8048	23.1770	0.0032
69	180	80	0.1000	0.5500	90	90	1.9895	14.5030	0.0276
70	197	80	0.1000	0.5500	0	0	3.4865	17.3445	0.0060

surface plot Figure 4, shows all the three objective function and their dominance on each other objective.

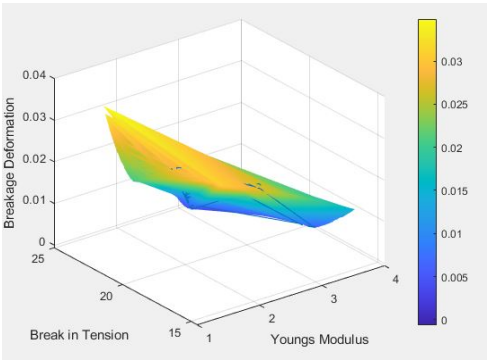

Figure 4 3-Dimensional Surface plot for three objectives

Table 3 Comparison of Optimized Value for Single and Multiple Objectives

	Breakage Deformation (mm)	Young's Modulus (GPa)	Breakage Tension (MPa)
Single objective	0.044	4.085	52.084
Multi-objective	0.032	3.5252	23.177
% Change	27.27	13.7	55.5

4.0 CONCLUSION

Optimum values of Young's modulus, breakage tension, and breakage deformation are obtained using a single objective function 'ga' in MATLAB. The results are tabulated in Tables, 1, 2, and 3. The optimum Youngs modulus, breakage tension, and breakage deformations are 4.045 GPa, 52.084 MPa, and 0.044 mm respectively. The input process parameters at these values are tabulated in Tables 1, 2, and 3. The input process parameters are different for optimum values of objectives such as Young's modulus, breakage tension, and breakage deformation as listed in Tables 1, 2, and 3.

Optimum values of Young's modulus, breakage tension, and breakage deformation are obtained using the multi-objective function 'gamultiobj' in MATLAB. This function simultaneously optimizes all three objectives which are dominating each other. Table 4 gives the optimum values of three objectives with their input process parameters. Though the simulation is set for 100 generations, it stopped at 70th generation due to no improvement in the results. The minimum value of breakage deformation is 0.0032 mm and the maximum value of breakage tension 23.177 Mpa is obtained at the 68th generation with the same input process parameters as shown in Table 4. However, the optimum Youngs modulus of 3.5252 GPa is obtained at the 16th generation with different input process parameters as tabulated in Table 4. Figures, 2 and 3 depict the minimum penalty values, best input parameters, and stopping of simulation details for a single objective function. However, Figure 4 indicates the surface plot considering all three objective function and their dominance over each other. In engineering applications where only the Youngs modulus is significant enough to withstand the load in the elastic condition, the input parameter as shown in Table 1 is suggested. But in many cases, deformation is the crucial factor which is as minimal as possible. Hence, the input process parameter as indicated in Table 3 would be appropriate. Though the Young's modulus is higher in the 16th generation as shown in Table 4, considering the importance of minimum deformation, the 68th generation is suggested where in breakage tension is also optimum at this input process parameter. Table 5 shows a comparison of the percentage of change of optimized values for single and multi-objectives at minimum deformation for multi-objective functions. This study reveals that simultaneously optimization of three objectives reduces a 27.27% breakage deformation, 13.7% Young's modulus, and 55.5% breakage tension as compared to the optimization of individual objectives.

Acknowledgements

The authors thank the organization for supporting this research work.

Conflicts of Interest

The author(s) declare(s) that there is no conflict of interest regarding the publication of this paper

References

[1] Drumright, R. E., Gruber, P. R., & Henton, D. E. 2000. Polylactic acid technology. *Advanced materials*. 12(23): 1841-1846. DOI: https://doi.org/10.1002/1521-4095(200012)12:23<1841::AID-ADMA1841>3.0.CO;2-E

[2] Averett, R. D., Realff, M. L., Jacob, K., Cakmak, M., & Yalcin, B. 2011. The mechanical behavior of poly (lactic acid) unreinforced and nanocomposite films subjected to monotonic and fatigue loading conditions. *Journal of composite materials*, 45(26): 2717-2726. DOI: https://doi.org/10.1177/0021998311410464

[3] Farah, S., Anderson, D. G., & Langer, R. 2016. Physical and mechanical properties of PLA, and their functions in widespread applications—A comprehensive review. *Advanced drug delivery reviews*, 107: 367-392. DOI: http://dx.doi.org/10.1016/j.addr.2016.06.012

[4] Mirkhalaf, S. M., & Fagerström, M. 2021. The mechanical behavior of polylactic acid (PLA) films: fabrication, experiments and modelling. *Mechanics of Time-Dependent Materials*, *25*(2): 119-131. DOI: https://doi.org/10.1007/s11043-019-09429-w

[5] Gibson, I., Rosen, D. W., & Stucker, B. 2010. *Additive manufacturing technologies: 3D printing, rapid prototyping, and direct digital manufacturing*. Springer Science & Business Media. (ISBN:1493921126)

[6] Hopkinson, N., Hague, R., & Dickens, P. 2006. *Rapid manufacturing: An industrial revolution for the digital age*. John Wiley & Sons.

[7] Saquib Rouf, Ankush Raina, Mir Irfan Ul Haq, Nida Naveed, Sudhanraj Jeganmohan, Aysha Farzana Kichloo, 2022. 3D printed parts and mechanical properties: Influencing parameters, sustainability aspects, global market scenario, challenges and applications, *Advanced Industrial and Engineering Polymer Research*. 5(3): 143-158. DOI: https://doi.org/10.1016/j.aiepr.2022.02.001

[8] Elisabetta Monaldo, Maurizio Ricci, Sonia Marfia. 2023. Mechanical properties of 3D printed polylactic acid elements: Experimental and numerical insights. *Mechanics of Materials.* 177: 104551. DOI: https://doi.org/10.1016/j.mechmat.2022.104551

[9] Travieso-Rodriguez, J.A., Jerez-Mesa Ramon, Jordi Llumà, Oriol Traver Ramos, Gómez-Gras, Giovanni, Joan Josep Roa Rovira. 2019. Mechanical Properties of 3D-Printing Polylactic Acid Parts subjected to Bending Stress and Fatigue Testing. *Materials*. 12(23): 3859. DOI: https://doi.org/10.3390/ma12233859

[10] Sandanamsamy L., Mogan J., Rajan K., Harun W. S. W., Ishak I., Romlay F. R., M. Samykano, Kadirgama K. 2023. Effect of process parameter on tensile properties of FDM printed PLA. *Materials Today: Proceedings*. DOI: https://doi.org/10.1016/j.matpr.2023.03.217

[11] Luca Fontana, Paolo Minetola, Luca Iuliano, Serena Rifuggiato, Mankirat Singh Khandpur, Vito Stiuso. 2022. An investigation of the influence of 3D printing parameters on the tensile strength of PLA material, *Materials Today: Proceedings.* 57(2): 657-663, DOI: https://doi.org/10.1016/j.matpr.2022.02.078

[12] Tofail S. A. M., Koumoulos E. P., Bandyopadhyay A., Bose S., O'Donoghue L., Charitidis C. 2018. Additive manufacturing: scientific and technological challenges, market uptake and opportunities. *Materials Today.* 21(1): 22-37. DOI: https://doi.org/10.1016/j.mattod.2017.07.001

[13] Kumar K. R., Mohanavel V., Kiran K. 2022. Mechanical properties and characterization of polylactic acid/carbon fiber composite fabricated by fused deposition modeling. *Journal of Materials Engineering and Performance*, 31(6): 4877-4886.

[14] Marşavina L., Vălean C., Mărghitaş M., Linul E., Razavi N., Berto F., Brighenti R. 2022. Effect of the manufacturing parameters on the tensile and fracture properties of FDM 3D-printed PLA specimens. *Engineering Fracture Mechanics.* 274: 108766.

[15] Tünçay M.M. 2024. An Investigation of 3D Printing Parameters on Tensile Strength of PLA Using Response Surface Method. *Journal of Materials Engineering and Performance*.33: 6249–6258. DOI: https://doi.org/10.1007/s11665-023-08395-2

[16] Ambade V., Rajurkar S., Awari G., B. Yelamasetti, S. Shelare. 2023. Influence of FDM process parameters on tensile strength of parts printed by PLA material. *International Journal on Interactive Design and Manufacturing.* DOI: https://doi.org/10.1007/s12008-023-01490-7

[17] Saifuddin Khan, Ketan Joshi, Samadhan Deshmukh. 2022. A comprehensive review on effect of printing parameters on mechanical properties of FDM printed parts. *Materials Today: Proceedings.* 50(5): 2119-2127, DOI: https://doi.org/10.1016/j.matpr.2021.09.433.

[18] Kumaresan R., Samykano M., Kadirgama K., Pandey A. K., Rahman M. M. 2023. Effects of printing parameters on the mechanical characteristics and mathematical modeling of FDM-printed PETG. *The International Journal of Advanced Manufacturing Technology*, *128*(7-8): 3471-3489. DOI: https://doi.org/10.1007/s00170-023-12155-w

[19] Manav Doshi, Ameya Mahale, Suraj Kumar Singh, Samadhan Deshmukh. 2022. Printing parameters and materials affecting mechanical properties of FDM-3D printed Parts: Perspective and prospects. *Materials Today: Proceedings*. 50(5): 2269-2275. DOI: https://doi.org/10.1016/j.matpr.2021.10.003.

[20] Kristiawan R. B., Imaduddin F., Ariawan D., Ubaidillah Arifin Z. 2021. A review on the fused deposition modeling (FDM) 3D printing: Filament processing, materials, and printing parameters. *Open Engineering*, 11(1): 639-649. DOI: https://doi.org/10.1515/eng-2021-0063

[21] Dey A., & Yodo N. 2019. A systematic survey of FDM process parameter optimization and their influence on part characteristics. *Journal of Manufacturing and Materials Processing*, *3*(3): 64. DOI: https://doi.org/10.3390/jmmp3030064

[22] Camposeco-Negrete C. 2020. Optimization of printing parameters in fused deposition modeling for improving part quality and process sustainability. *The International Journal of Advanced Manufacturing Technology.* 108(7): 2131-2147. DOI: https://doi.org/10.1007/s00170-020-05555-9

[23] Kafshgar A. R., Rostami S., Aliha M. R. M., Berto, F. 2021. Optimization of properties for 3D printed PLA material using taguchi, anova and multi-objective methodologies. *Procedia Structural Integrity.* 34: 71-77. DOI: https://doi.org/10.1016/j.prostr.2021.12.011

[24] Yodo N., & Dey A. 2021. Multi-objective optimization for FDM process parameters with evolutionary algorithms. *Fused Deposition Modeling Based 3D Printing.* 419-444. DOI: https://doi.org/10.1007/978-3-030-68024-4_22

[25] Raghavendra B. 2020. Hybrid genetic algorithm for bi-criteria objectives in scheduling process. *Management and Production Engineering Review,* 11. DOI: 10.24425/mper.2020.133733

[26] Raghavendra B.V. 2019. Effect of Crossover Probability on Performance of Genetic Algorithm in Scheduling of Parallel Machines for BI- Criteria Objectives. *International Journal of Engineering and Advanced Technology.* 9(1): 2827–2831. DOI: 10.35940/ijeat.A9801.109119

[27] Puttaswamy S., & Raghavendra V. 2021. Effect of Machining Parameters On Surface Roughness, Power Consumption, and Material Removal Rate of Aluminium 6065-Si-Mwcnt Metal Matrix Composite In Turning Operations. *IIUM Engineering Journal.* 22(2): 283–293. DOI: https://doi.org/10.31436/iiumej.v22i2.1640

[28] Eguren J.A., Esnaola A., & Unzueta G. 2020. Modelling of an additive 3D-printing process based on design of experiments methodology. *Quality Innovation Prosperity.* 24(1): 128-151. DOI: https://doi.org/10.12776/qip.v24i1.1435